UDC 541.6:541.67

INTRAMOLECULAR-PROTON TRANSFER, EXPERIMENTAL AND THEORETICAL CHARACTERIZATION OF 3,3′-DIHYDROXY-4,4′-[4,4′-DIPHENYLMETHANEBIS (NITRILOMETHYLIDYNE)]-BIS-PHENOL

H. Eshtiagh-Hosseini[1], S.A. Beyramabadi[2], M. Mirzaei[1], A. Morsali[2], M.A. Naseri[3], H. Chegini[2], M. Elahi[2]

[1]*Department of Chemistry, Ferdowsi University of Mashhad, Mashhad, Iran*
[2]*Department of Chemistry, Mashhad branch, Islamic Azad University, Mashhad, Iran*
  E-mail: beiramabadi6285@mshdiau.ac.ir
[3]*Department of Chemistry, Faculty of Science, Birjand University, Birjand, Iran*

A newly synthesized Schiff base 3,3′-dihydroxy-4,4′-[4,4′-diphenylmethanebis(nitrilomethylidyne)]-bis-phenol is characterized experimentally. Also, the geometry optimization for the tautomers, tautomerism and assignment of the IR bands and NMR chemical shifts of the Schiff base were performed using the DFT method. Good consistency between the theoretical and experimental results confirms the validity of the optimized geometry. Geometries of four possible tautomers are fully optimized. None of them has a planar structure, but each of the benzene rings is in a separate plane. In the most stable tautomer **L1**, the phenolic protons are engaged in the intramolecular-hydrogen bond with the azomethine nitrogen atoms. Tautomerization of **L1** can occur in two different pathways which are computationally studied using DFT and the Atoms In Molecules (AIM) analysis. Both pathways have the same barrier energy.

INTRODUCTION

The syntheses of salen and salophen ligands along with their complexes have received much attention due to their extensive applications, especially in the field of biochemistry and catalysis [1—4].

Transition metal salen complexes are recognized as powerful homogeneous catalysts in the oxidation reactions. The Schiff base complexes have mainly been used as DNA cleavage catalysts [5—11].

In continuation of our previous works on the chemistry of Schiff bases [12—18], herein we report the synthesis, experimental and theoretical investigation of a new Schiff-base (3,3′-dihydroxy-4,4′-[4,4′-diphenylmethanebis(nitrilomethylidyne)]-bis-phenol), which is named as **L**. By comparing the theoretical and experimental results, the validity of the optimized structures has been evaluated.

EXPERIMENTAL

Materials and methods. All of used chemicals were purchased from Merck Company and used as recieved. Melting points were determined using an electrothermal 9100 melting point apparatus. The IR spectra were recorded on a Buck 500 IR spectrophotometer. Elemental analysis (C, H, N) was performed on a Heraeus CHN-O-Rapid elemental analyzer. The ^{1}H and ^{13}C NMR spectra were re-

corded on a Bruker Drx-500 Avance spectrometer (500.13 MHz), with DMSO as a solvent. Mass spectra were scanned on Shimadzu-GC-Mass-Qp 1100 Ex.

Synthesis of the titled Schiff base ($C_{27}H_{22}N_2O_4$). A solution of 1.32 g (6.66 mmol) of 4-(4-aminobenzyl)benzenamine and 1.88 g (13.61 mmol) of dihydroxybenzaldehyde in toluene (150 ml) was refluxed under vigorous stirring with a Dean-Stark for 3 h. The resulting suspension was kept at room temperature prior to being filtered, washed with ethanol (2×10 ml), and dried with diethyl ether (2×10 ml) to afford a red solid. The solid was recrystallized for further purification. (Yield: 58 %, m.p. > 250°C, Anal. Calcd. (%) for $C_{20}H_{20}N_2O_4$: C 70.39, H 6.16, N 7.14. Found: C 67.68, H 4.89, N 8.28, the molecular ion peaks, m/z (M^+) = 438).

COMPUTATIONAL DETAILS

All calculations have been performed using density functional theory with the B3LYP functional [19] as implemented in the Gaussian 03 program package [20]. The 6-311+G(d,p) basis set was employed.

Firstly, all of the geometries were fully optimized. The optimized geometries were confirmed to have no imaginary frequency of the Hessian, which was used for the additional calculations, including the frequencies, NMR chemical shifts, and AIM calculations. The ^{1}H and ^{13}C NMR chemical shifts of the **L** species were predicted with respect to tetramethylsilane (TMS). Here, the GIAO method was used for the prediction of DFT nuclear shieldings [21]. The DFT-predicted vibrational frequencies are usually higher than the experimental ones scaled here by a factor of 0.9614 [22].

The AIM topological analyses were carried out in accordance with Bader′s approach [23] using the AIMall package [24]. The DENSITY = CURRENT option was used to generate the wave function files.

RESULTS AND DISCUSSION

Geometry optimization. Considering two intramolecular proton transfers, there are four possible tautomers for the titled Schiff base, geometries of which are optimized in both gas and solution phases. The PCM model was used for considering the solvent effects. **L1** is the most stable tautomer, where the H1 and H2 atoms are bonded to the phenolic O1 and O2 atoms. The **L1** tautomeric form is more stable than the **L2**, **L3** and **L4** tautomers by 12.52 kJ/mol^{-1}, 11.70 kJ/mol^{-1}, and 11.82 kJ/mol^{-1} respectively.

In this work, the structural parameters of the **L1** Schiff base have been calculated theoretically, and some of them are gathered in Table 1. The obtained results are in agreement with the structural data reported for the similar compounds [12—18, 25—31]. The optimized geometry of the investigated Schiff base with its atom labeling is shown in Fig. 1.

The elemental analysis results for the titled Schiff base confirm the proposed formula.
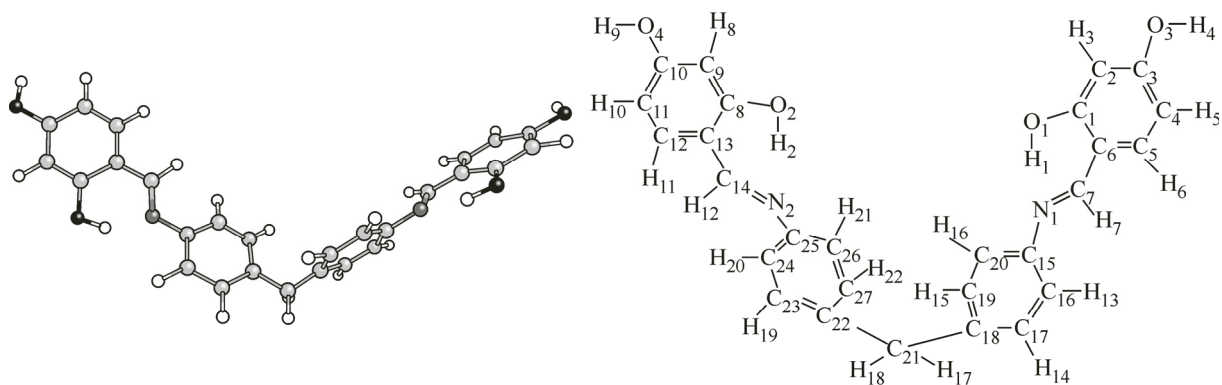

Fig. 1. Structure and B3LYP optimized geometry of **L1** together with its labeling

T a b l e 1

Selected structural parameters of
3,3′-dihydroxy-4,4′-[4,4′-diphenylmethanebis(nitrilomethylidyne)]-bis-phenol

Bond length, pm		Angle, deg.		Dihedral angle, deg.	
O1—H1	99.5	H1—O1—C1	107.5	H1—O1—C1—C2	179.6
H1—N1	173.6	N1—H1—O1	147.8	C1—C2—C3—C4	0.1
N1—O1	263.2			C2—C3—O3—H4	−180.0
C1—O1	133.9	O1—C1—C2	118.5	C2—C3—C4—H5	180.0
C1—C2	139.5	C1—C2—C3	119.9	O1—C1—C6—C7	−0.1
O3—H4	96.3	C2—C3—O3	117.1	C1—C6—C7—N1	0.5
C4—H5	108.5	O1—C1—C6	121.4	C6—C7—N1—C15	−177.1
C6—C7	144.4	C1—C6—C7	121.6	C7—N1—C15—C16	−145.7
C7—H7	109.6	C6—C7—N1	122.5	C15—C16—C18—C19	1.2
C7—N1	129.0	C7—N1—C15	121.2	C16—C17—C18—C21	178.2
N1—C15	140.7	N1—C15—C16	118.2	C17—C18—C21—C22	57.8
C15—C16	140.3	C15—C16—C17	120.6	C1—O1—O2—C8	−57.1
C18—C21	151.8	C18—C21—C22	114.8	C4—C1—C8—C11	−55.1
N1—N2	976.6	C3—O3—H4	109.9	C16—C19—C27—C24	162.8
O1—O2	1445.2			C7—N1—N2—C14	−52.8
O1—N1	259.9			C2—C1—C9—C8	126.3
				C1—C5—C16—C20	37.3

In the optimized geometry of **L1**, the C=C bond lengths (138.2—142.5 pm) of the benzene rings are in the expected range. The benzene rings are essentially planar, but each of them lies in a separate plane which make a dihedral angle of approximately 45° to each other. For example, the C4—C3—C9—C10 dihedral angle is −45.1°.

The resorcinol OH groups are in the same plane with the benzene ring (Table 1). The H1 and H2 atoms are engaged in intramolecular hydrogen bonds with the azomethine nitrogen atoms (N1 and N2 atoms, respectively), forming two six-membered rings. The calculated N…H hydrogen bond length and N—O distance are 173.6 pm and 263.2 pm, respectively. The Electron density in the binding region of the O1—H1 and O2—H2 bonds decreases due to these hydrogen bonding interactions. Therefore, the O1—H1 and O2—H2 bonds are longer than the O3—H4 and O4—H9 bonds (by 3.2 pm) not engaged in the intramolecular H-bonds.

In the diamine-bridge region, two benzene rings are at a dihedral angle of 60° to each other. The calculated C16—C20—C27—C23, C16—C17—C22—C25 dihedral angles are −59.0 and −67.0°, respectively.

Both C15—N1 and C25—N2 bond lengths are of appropriate size for the single C—N bond, while both azomethine C7—N1 and C14—N2 bonds correspond to the double C=N bond. The C7=N1 and C14=N2 bonds are in the same plane with the corresponding benzene rings.

The DFT calculated parameters for the investigated Schiff base are consistent with the previously reported data for the similar salen ligands and complexes [12—18, 25—31].

NMR spectrum. Theoretical and experimental ^{1}H and ^{13}C NMR chemical shifts (δ) of the **L1** species are listed in Table 2, where the atom positions are numbered as in Fig. 1. The calculated chemical shifts are in agreement with the experimental ones, confirming the suitability of the optimized geometry for the **L** Schiff base. The only exceptions are the H4 and H9 hydrogen atoms, where the calculated chemical shifts are significantly lower than the experimental ones. It is notable that the experimental data are from DMSO solutions; while the calculated results correspond to the isolated molecule in the gas phase. Obviously, the solvent molecules interact with the —OH protons. In addition, the H4 and H9 atoms can be engaged in intermolecular hydrogen bonds.

T a b l e 2

Experimental and DFT *computed* ^{1}H *and* ^{13}C NMR *chemical shifts of*
3,3′-*dihydroxy*-4,4′-[4,4′-*diphenylmethanebis*(*nitrilomethylidyne*)]-*bis-phenol in a* DMSO *solution*, δ (ppm)

^{1}H NMR						^{13}C NMR					
Atom position	Exp.	Theor.	Atom position	Exp.	Theor.	Atom position	Exp.	Theor.	Atom position	Exp.	Theor.
H1	13.60	13.01	H15	7.30	7.22	C1	163.4	172.11	C17	134.7	134.98
H2	13.60	13.01	H19	7.30	7.22	C8	163.4	171.91	C27	134.7	134.06
H4	10.24	3.94	H22	7.30	7.22	C10	162.7	167.48	C20	130.0	131.29
H9	10.24	3.94	H16	7.30	7.06	C3	162.7	167.37	C26	130.0	129.44
H7	8.80	8.52	H21	7.30	7.06	C7	162.4	164.70	C24	121.5	121.81
H12	8.80	8.36	H3	6.35	6.71	C14	162.4	164.70	C16	121.5	120.08
H20	7.42	7.48	H8	6.35	6.66	C15	146.4	155.61	C6	112.4	118.80
H13	7.42	7.38	H10	6.29	5.96	C25	146.4	154.82	C13	112.4	118.60
H6	7.30	7.22	H5	6.29	5.91	C18	146.4	147.38	C4	108.2	107.61
H11	7.30	7.22	H17	3.97	3.71	C22	146.4	147.38	C11	108.2	107.30
H14	7.30	7.22	H18	3.97	3.71	C5	139.8	138.32	C2	102.7	106.95
						C12	139.8	138.09	C9	102.7	106.95
						C19	134.7	135.68	C21	45	45.21
						C23	134.7	135.51			

A signal at 13.60 ppm is related to the H1 and H2 phenolic protons (H1, H2). Their engagement in the intramolecular hydrogen bond interaction (O—H…N), shifts their signals upfield [12—18, 32].

Vibrational spectroscopy. Nowadays, a theoretical assignment of the spectra provides a quantitative framework for the understanding and identification of chemical compounds [12—18, 33—35]. In addition to the NMR chemical shifts, the vibrational modes were analyzed by comparing the DFT and experimental IR spectra. The obtained DFT results could be useful in the identification of similar compounds.

The assignment of the selected vibrational frequencies of the most stable tautomer of the titled Schiff base **L1** is gathered in Table 3. The broad bond in the 3600—2000 cm^{-1} spectral region is attributed to the overlap of the O—H and C—H stretching vibrations [12—18, 36, 37]. The deconvolution of this region is given in Table 3. The most intense band is related to the stretching vibrations of the O1—H1 and O2—H2 bonds. These vibrations appear at much lower energies than the corresponding vibrations for the O3—H4 and O4—H9 bonds due to the engagement of H1 and H2 in the intramolecular hydrogen bonds.

The very intense band in the 1660—1500 cm^{-1} region is attributed to the azomethine C=N bonds. Also, the C—O stretching vibrations result in strong bands [12—18, 36, 37]. These two important bands appear at 1624 cm^{-1} and 1250 cm^{-1}, respectively.

Electrostatic potential map. In the structure of the titled Schiff base there are two possible sites (1 and 2) for the intramolecular proton transfer (IPT) as N…OH between the phenolic —OH group and the azomethine N atom. Both 1 and 2 sites seem similar, but the IPT can only occur in site 1, which will be explained below.

The electrostatic potentials V_S (*r*), of the **L1**, **L2**, **L3**, and **TSL1—L2** species are shown in Fig. 2, where the negative and positive potentials are shown in red and blue colors, respectively.

As shown in Fig. 2, there is a region of positive V_S (*r*) in the most external part of H21 (the region located in the continuation of O8—H21) in the overall structure, but a more negative potential in the **L1** and **L3** area of the structure is very prominent. This shows that going from the **L1** and **L3**, IPT occurs through site 1 [38]. The negative V_S (*r*) is located at the outermost part of N25. The interaction between the negative V_S (*r*) region of N25 and the positive V_S (*r*) region of H45 is one of the reasons for the intramolecular hydrogen bond formation of **L1**.

T a b l e   3

Selected experimental and calculated IR vibrational frequencies (cm^{-1}) *of*
3,3′-dihydroxy-4,4′-[4,4′-diphenylmethanebis(nitrilomethylidyne)]-bis-phenol

Experimental frequencies	Calculated frequencies	Vibrational assignment
831(m)	845	δ_{op}(O1—H1, O2—H2)
	953	Breathing of benzene rings
1128 (s)	1147	δ_{ip}(aromatic hydrogens)
1170(s)	1176	ν_{asym}(C18—C21—C22)
1190(s)	1225	ν(C6—C7, C13—C14, C15—N1, C25—N2)
1250(s)	1289	ν(C—O)
	1305	δ_{wag}(CH$_2$)
1330 (s)	1342	δ_{ip}(C7—H7, C14—H12)
1467(m)	1428	ν(C1—O1, C8—O2)
1514(s),1600(vs)	1486, 1578	ν_{sym}(C=C) benzene rings
1624(vs)	1600	ν(C7=N1, C14=N2)
2960(sh), 3423(br)	2903	ν_{sym}(C21—H)
	2919	ν(C7—H7, C14—H12)
	2934	ν_{asym}(C21—H)
	3051	ν(O1—H1, O2—H2)
	3034—3051	ν(C—H) aromatic
	3085	ν(C2—H3, C9—H8)
	3684	ν(O3—H4, O4—H9)

A b b r e v i a t i o n s: op — out-of-plane; ip — in-plane; sh — shoulder; w — weak;
m — medium; s — strong; vs — very strong; br — broad.

Topological analysis. The Bader theory is a very suitable tool for analyzing hydrogen bonds. The analysis of the properties of BCPs has often been used as the evaluation of the nature of hydrogen bonds [39—41]. Fig. 2 presents examples of optimized systems, including keto-amine (with the N—H…O hydrogen bond), its enol-imine tautomeric form (with O—H…N hydrogen bond), and the transition state of the corresponding proton transfer reaction in three pathways.

The parameters derived from the Bader theory, for example, the Laplacian of the electron density $\nabla^2\rho$, local electron energy densities of HC and its components at BCPs are also indicators for the strength of the H bonds [41, 42]. The electron energy density (HC), the sum of the kinetic electron energy density (GC), the potential electron energy density (VC), and –GC/VC indicate the interaction type. For a negative value of the Laplacian, the interaction or the bond will doubtlessly be covalent.

If $\nabla^2\rho$ and HC are positive, the interaction is noncovalent. If $\nabla^2\rho$ is positive but HC is negative, and –GC/VC is smaller than 1, then the interaction may be classified as partly covalent in nature [38, 42].

The typical topological parameters at H$\cdots$Y BCP is 0.002—0.04 a.u. for the electron density and 0.02—0.15 a.u. for its Laplacian. [16, 39, 40]. The obtained results for all O—H…N systems analyzed here are as follows: the electron densities at H…O BCPs — ρ H…O are higher than these densities at H…N BCPs — ρ H…N of O—H…N hydrogen bonds. Additionally, all the HC values of the BCPs (of H…N contacts) are negative, indicating the partly covalent character of these interactions.

The topological parameters, such as $\nabla^2\rho_{BCP}$, $\nabla^2\rho$, GC, VC, and HC at the BCP of N…HO, O…HN bonds in two sites of the intramolecular hydrogen bonds are listed in Table 4.
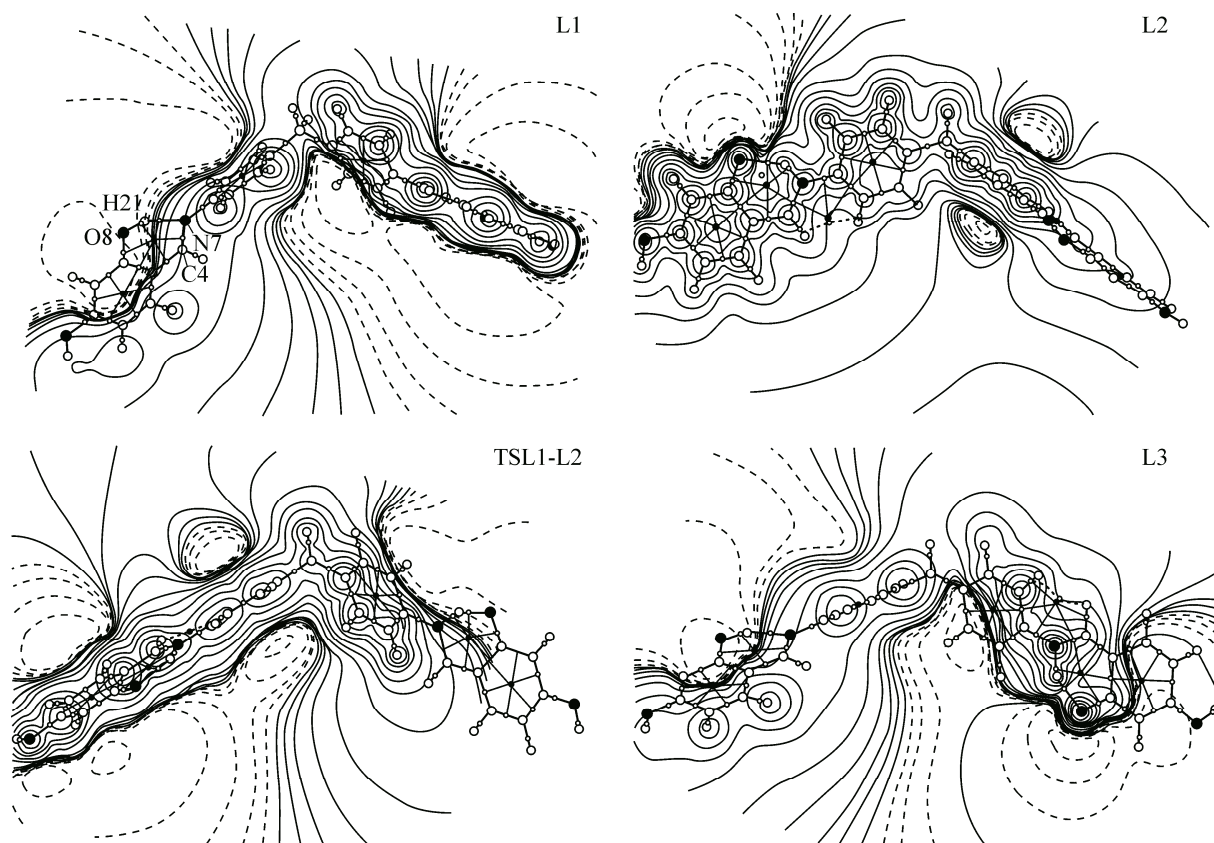
Fig. 2. Electrostatic potential map of the studied species

T a b l e   4

Topological properties at the BCP *of* N…HO *and* NH…O *bonds in the*
L1, L3, L4, L2, TsL1—L3, TsL1—L4, TsL1—L2, TsL3—L2, TsL4—L2 *species*

Species	Site1							
	BPL	Bond	ρ	∇2ρ	GC	VC	HC	–GC/VC
L1	0.972117	O8—H21	0.327138	–2.25282	0.068845	–0.70089	–0.63205	0.098225
	1.75772	N7—H21	0.050205	0.111191	0.037127	–0.04646	–0.00933	0.799169
L2	1.706382	O8—H21	0.051589	0.146152	0.042923	–0.04931	–0.00639	0.87049
	1.024362	N7—H21	0.307863	–1.61499	0.048138	–0.50002	–0.45188	0.096272
L3	0.971993	O8—H21	0.327275	–2.25399	0.068883	–0.70126	–0.63238	0.098227
	1.757411	N7—H21	0.050239	0.111324	0.037174	–0.04652	–0.00934	0.799149
L4	1.708572	O8—H21	0.051326	0.145851	0.042711	–0.04896	–0.00625	0.872365
	1.024096	N7—H21	0.308086	–1.61698	0.048075	–0.5004	–0.45232	0.096074
TSL1—L2	1.261562	C2—O8	0.367507	–0.38985	0.0898	–1.07976	–0.98996	0.083167
	1.024629	N7—H21	0.307505	–1.61211	0.068265	–0.49939	–0.43113	0.136697
TSL1—L3	0.971984	O8—H21	0.32728	–2.25422	0.068849	–0.70125	–0.6324	0.09818
	1.75803	N7—H21	0.050163	0.111241	0.037112	–0.04641	–0.0093	0.799604
TSL1—L4	1.288617	O8—H21	0.143774	–0.0319	0.089937	–0.18785	–0.09791	0.478775
	1.198821	N7—H21	0.194826	–0.48315	0.06832	–0.25743	–0.18911	0.265397
TSL3—L2	1.292231	O8—H21	0.142483	–0.02448	0.089613	–0.18535	–0.09573	0.483493
	1.195815	N7—H21	0.19614	–0.49476	0.068167	–0.26003	–0.19186	0.262156
TSL4—L2	1.706761	O8—H21	0.051543	0.146101	0.042888	–0.04925	–0.00636	0.870822
	1.024315	N7—H21	0.307912	–1.61528	0.04813	–0.50008	–0.45195	0.096244

О к о н ч а н и е т а б л. 4

Species	Site2							
	BPL	Bond	ρ	$\nabla 2\rho$	GC	VC	HC	–GC/VC
L1	0.971926	O32—H39	0.327322	–2.25519	0.068762	–0.70132	–0.63256	0.098046
	1.759848	N35—H39	0.049954	0.11107	0.036948	–0.04613	–0.00918	0.800971
L2	1.702914	O32—H39	0.051997	0.146674	0.043275	–0.04988	–0.00661	0.867547
	1.024607	N35—H39	0.307751	–1.61434	0.048233	–0.50005	–0.45182	0.096456
L3	1.707636	O32—H39	0.051439	0.146031	0.04281	–0.04911	–0.0063	0.871699
	1.024212	N35—H39	0.307896	–1.61554	0.048105	–0.5001	–0.45199	0.096192
L4	0.971646	O32—H39	0.327609	–2.25819	0.068748	–0.70204	–0.6333	0.097925
	1.760787	N35—H39	0.049829	0.111136	0.036887	–0.04599	–0.0091	0.802048
TSL1—L2	1.29046	O32—H39	0.143119	–0.028	0.043096	–0.1866	–0.1435	0.230954
	1.197168	N35—H39	0.19556	–0.48948	0.048181	–0.2589	–0.21072	0.1861
TSL1—L3	1.289704	O32—H39	0.143373	–0.02969	0.089814	–0.18705	–0.09724	0.480163
	1.197992	N35—H39	0.195156	–0.48616	0.068264	–0.25807	–0.1898	0.26452
TSL1—L4	0.971631	O32—H39	0.32761	–2.25837	0.06873	–0.70205	–0.63332	0.097899
	1.761113	N35—H39	0.049793	0.111094	0.036857	–0.04594	–0.00908	0.802268
TSL3—L2	1.705088	O32—H39	0.051745	0.146386	0.043058	–0.04952	–0.00646	0.869525
	1.024498	N35—H39	0.307658	–1.61349	0.048178	–0.49973	–0.45155	0.096408
TSL4—L2	1.291752	O32—H39	0.142652	–0.02507	0.089714	–0.1857	–0.09598	0.483123
	1.195838	N35—H39	0.196134	–0.49435	0.068229	–0.26005	–0.19182	0.262372

The molecular graphs show the existence of a BCP between the H(21) and N(7) atoms and the H(35) and N(39) atoms linked by two bond paths. The topological structure indicates that the intramolecular hydrogen bond exists in **L1**. Table 4 shows that at the BCP of the hydrogen bond, $\nabla^2\rho$ is positive, while HC is negative, and the ratio of GC and VC (GC/VC) is between 0.5 and 1; all the topological parameters show that the intramolecular hydrogen bond is partly covalent [43].

In comparison with the other structures, ρ_{BCP} at the BCP is greater in **L1**, indicating the strongest hydrogen bond for **L1**. As compared with the **L1** tautomer, in the **L2**, **L3**, and **L4** ones, the absolute values of $\nabla^2\rho$, GC, VC, and HC increase while –GC/VC decreases, which means that the covalent portion increases in the **L2**, **L3**, and **L4** tautomers.

At the first look on the electrostatic potential map, site 1 shows a stronger H-bond than site 2; which is not clearly confirmed by Table 4 data. ρ_{BCP} at the BCP is expected to change in **L4** towards

T a b l e 5

Dihedral angles (Å) *in site 1 involving* C4—C15—C10—C53 *and in site 2 involving* C34—C43—C46—C53 *in all molecules and transition states*

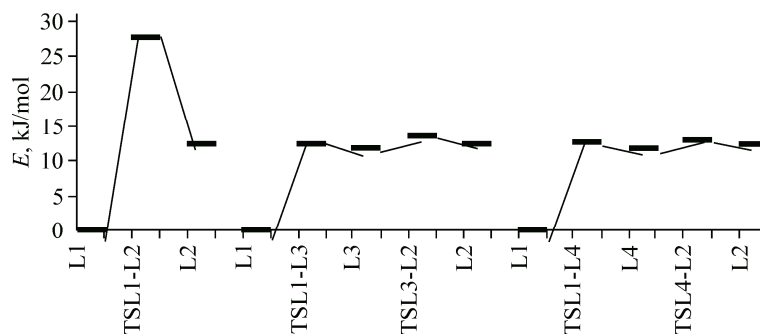| Species	C4—C15—C10—C53 (Site 1)	C34—C43—C46—C53 (Site 2)
L1	–2.3	2.3
L2	–101.4	91.2
L3	–123.5	69.4
L4	–93.2	129.0
TSL1—L2	36.9	88.7
TSL1—L3	–134.6	114.4
TSL1—L4	–63.1	131.5
TSL3—L2	–111.2	78.4
TSL4—L2	–101.7	68.9

Fig. 3. Relative energy diagram of the **L** tautomerization

ρ_{BCP} at the BCP in **L3**. Furthermore, the other parameters have been expected to have numerous changes. **L4** has a proton transfer at site 2, but the proton transfer of **L3** locates at site 1. The H…N BCPs — ρ H…N of the O—H…N hydrogen bond for **L3** and **L4** are 0.307896 and 0.308086, respectively. If we focus on the magnitudes of $\nabla^2\rho$ and HC, we see that all parameters have a negligible difference in **L3** and **L4** at BCP in the proton transfer bond path.

It is acceptable that two sites have the same opportunity of the intermolecular proton transfer. It is expected because of different dihedral angles of two sites, a distinctive electron density distribution, and different H-bond strengths. However, different H-bonds have not been seen at the two sites, so the dihedral angle has no effect on the proton transfer, which is in good agreement with the energy diagram (Fig. 3).

AIM analysis at RCP. The RCP is a point of the minimum electron density within the ring surface and the maximum on the ring line [44]. The intramolecular hydrogen bond forms a H—O—C=C—C—N ring. Table 6 gives the electron density ρ_{BCP} at the RCP and $\nabla^2\rho$ of this ring. The difference between the RCP and the BCP of the hydrogen bond is also listed in Table 6.

The extended $d_{RCP \to BCP}$ implies that the hydrogen bond becomes stronger in the **L1** tautomer. This as well means that the properties of RCP (ρ_{RCP} and $\nabla^2\rho$) could probably be treated as measures of the intramolecular hydrogen bond strength. The $d_{RCP \to BCP}$ is a good descriptor for explaining the hydrogen bond strength. We see that two sites have the same rule for changing values, but have negligible changes in ρ_{RCP} that could be affected by the electron deloclization in the ring line, which will be explained below.

Delocalization index. According to Fradera et al. [45], the electron delocalization index (DI) (the average number of electrons delocalized between the bonded A and B atoms) is an evaluation of

T a b l e 6

Topological properties at the RCP, *the difference between the* RCP *and the* BCP *in the studied species*

Species	Site 1			Site 2		
	ρ	$\nabla 2\rho$	dRCP-bcp	ρ	$\nabla 2\rho$	dRCP-bcp
L1	0.018039	0.113238	0.820124	0.018009	0.112974	0.819636
L2	0.017976	0.117117	0.838655	0.018023	0.11754	0.838925
L3	0.018038	0.113271	0.820259	0.017963	0.117011	0.838511
L4	0.017949	0.116871	0.83814	0.017992	0.112867	0.819364
TsL1—L2	0.018003	0.117351	0.839279	0.02314	0.157978	0.950622
TsL1—L3	0.018032	0.113198	0.820068	0.023143	0.158003	0.920559
TsL1—L4	0.023154	0.158056	0.950021	0.017987	0.112825	0.819301
TsL3—L2	0.021554	0.157623	0.951166	0.017996	0.117305	0.839035
TsL4—L2	0.017971	0.117074	0.838551	0.023136	0.157983	0.920441

T a b l e 7

Electron delocalization index (*average number of electrons delocalized between* A *and* B *atoms*). *q*(A|B) *Contribution of the bond between* A *and* B *atoms to q*(A) *and* BPL *is the bond path length of* A *and* B *atoms*

Species	Site 1				Site 2			
	Bond	q(A|B)	DI (A, B)	BPL	Bond	q(A|B)	DI (A, B)	BPL
1	2	3	4	5	6	7	8	9
L1	C4—N7	0.691	1.4711	1.290822	C34—N35	0.6899	1.4713	1.153422
	C1—C4	0.0332	1.1242	1.444276	C30—C34	0.0332	1.1246	1.290468
	C1—C2	0.0257	1.2009	1.425262	C27—C30	0.0263	1.2008	1.273599
	C2—O8	0.6053	0.9953	1.338791	C27—O32	0.6048	0.9956	1.196265
	O8—H21	0.5304	0.4877	0.972117	O32—H39	0.5307	0.4881	0.868495
	N7—H21	0.0866	0.1295	1.75772	N35—H39	0.0862	0.1291	1.572567
L2	C4—N7	0.4189	1.2137	1.331343	C34—N35	0.42	1.2135	1.189606
	C1—C4	0.1438	1.3307	1.392465	C30—C34	0.1417	1.3314	1.244299
	C1—C2	0.0972	1.0561	1.473851	C27—C30	0.0955	1.0555	1.317325
	C2—O8	0.9726	1.2326	1.261269	C27—O32	0.9717	1.233	1.126997
	O8—H21	0.1702	0.137	1.706382	O32—H39	0.1706	0.1376	1.521692
	N7—H21	0.3353	0.5968	1.024362	N35—H39	0.3353	0.5955	0.91557
L3	C4—N7	0.6934	1.4694	1.291045	C34—N35	0.4165	1.2163	1.189082
	C1—C4	0.0356	1.1258	1.443891	C30—C34	0.1476	1.3284	1.244603
	C1—C2	0.0263	1.2005	1.425453	C27—C30	0.0984	1.0567	1.316816
	C2—O8	0.606	0.9955	1.338783	C27—O32	0.972	1.2327	1.127164
	O8—H21	0.5295	0.4879	0.971993	O32—H39	0.1709	0.1366	1.525911
	N7—H21	0.0873	0.1294	1.757411	N35—H39	0.3348	0.5971	0.915216
L4	C4—N7	0.4151	1.2156	1.330888	C34—N35	0.6931	1.4699	1.153557
	C1—C4	0.1488	1.3289	1.392789	C30—C34	0.0366	1.1256	1.290184
	C1—C2	0.0992	1.0568	1.473646	C27—C30	0.0278	1.2004	1.273685
	C2—O8	0.9721	1.2338	1.261301	C27—O32	0.6051	0.9956	1.196221
	O8—H21	0.171	0.1363	1.708572	O32—H39	0.53	0.4884	0.868245
	N7—H21	0.3346	0.5974	1.024096	N35—H39	0.0871	0.1286	1.573406
TSL1—L2	C4—N7	0.4185	1.2152	1.331003	C34—N35	0.4185	1.2152	1.189359
	C1—C4	0.1453	1.3295	1.392663	C30—C34	0.1453	1.3295	1.244457
	C1—C2	0.0976	1.0567	1.473722	C27—C30	0.0976	1.0567	1.31689
	C2—O8	0.9716	1.2323	1.261562	C27—O32	0.9716	1.2323	1.127308
	O8—H21	0.9716	1.2323	1.261562	O32—H39	0.3315	0.2877	1.153131
	N7—H21	0.3348	0.596	1.024629	N35—H39	0.2327	0.3843	1.069766
TSL1—L3	C4—N7	0.6927	1.4701	1.290932	C34—N35	0.5372	1.3247	1.173141
	C1—C4	0.0348	1.1249	1.444052	C30—C34	0.0669	1.2329	1.263395
	C1—C2	0.026	1.2007	1.425338	C27—C30	0.0349	1.1175	1.297269
	C2—O8	0.6056	0.9956	1.338802	C27—O32	0.7977	1.1296	1.155509
	O8—H21	0.5299	0.488	0.971984	O32—H39	0.333	0.2881	1.152455
	N7—H21	0.087	0.1294	1.75803	N35—H39	0.2313	0.3838	1.070503
TSL1—L4	C4—N7	0.5373	1.3247	1.312859	C34—N35	0.6923	1.4705	1.153466
	C1—C4	0.067	1.2322	1.41402	C30—C34	0.0356	1.1251	1.290302
	C1—C2	0.0351	1.1178	1.451688	C27—C30	0.0274	1.2006	1.273641
	C2—O8	0.7973	1.1287	1.293237	C27—O32	0.6048	0.9956	1.196229
	O8—H21	0.3338	0.2886	1.288617	O32—H39	0.5303	0.4884	0.868231
	N7—H21	0.2306	0.3832	1.198821	N35—H39	0.0868	0.1286	1.573697

1	2	3	4	5	6	7	8	9
TSL3—L2	C4—N7	0.5395	1.322	1.313404	C34—N35	0.4188	1.2148	1.189409
	C1—C4	0.0648	1.2348	1.413336	C30—C34	0.1441	1.3302	1.244349
	C1—C2	0.0354	1.1168	1.452027	C27—C30	0.0969	1.0562	1.317081
	C2—O8	0.8002	1.1302	1.292914	C27—O32	0.9717	1.2329	1.127138
	O8—H21	0.3306	0.2871	1.292231	O32—H39	0.1708	0.1372	1.523635
	N7—H21	0.2334	0.3854	1.195815	N35—H39	0.3353	0.5962	0.915472
TSL4—L2	C4—N7	0.4184	1.2142	1.331201	C34—N35	0.5396	1.3225	1.173565
	C1—C4	0.1452	1.33	1.392611	C30—C34	0.064	1.2351	1.262904
	C1—C2	0.098	1.0564	1.473759	C27—C30	0.0344	1.1166	1.297549
	C2—O8	0.9725	1.2327	1.261332	C27—O32	0.8001	1.1301	1.155254
	O8—H21	0.1705	0.1368	1.706761	O32—H39	0.3303	0.2871	1.154285
	N7—H21	0.335	0.5969	1.024315	N35—H39	0.2338	0.3851	1.068579

the variety of electron pairs shared by two basins; however, they do not declare this function to be a bond order; it is similar to the covalent order defined by Ánglyán et al. [46].

DIs between (H—) N—C, C=C, C—C and C=O or N=C, C—C, C=C and C—O (—H) in the chelate ring at both sites are listed in Table 7, which confirms the intramolecular hydrogen bond. Also, Table 7 shows the geometrical parameters of the investigated species. One can notice that the geometries indicate more impressive O—H…N interactions than N—H…O ones. Namely, the H…N distances within O—H…N bonds are regularly scaled-down by 1.75—1.57 Å, while the range of H…O distances in the N—H…O interaction is 1.52—1.70 Å. The shortest H…O and H…N contacts can be found in transition states. It can be supposed that the proton-acceptor distance is the rough evaluation of the hydrogen bonding strength [47].

There are conjugated single-double bonds: (H—) N—C, C=C, C—C, C=O or N=C, C—C, C=C, C—O (—H) that are more or less equalized due to the π electron delocalization (Table 7).

The events described here show that in the case of N—H…O intramolecular H bonds, the extra Lewis acid in proximity of the C=O proton acceptor causes an increase in Lewis base attraction of the oxygen atom and the weakening of the intramolecular H bond. All geometrical and topological data (Tables 6 and 7) establish these findings. The electron density increases at the N—H BCP; the H…O distance within the NH…O bridge is elongated and the electron density decreases at the H…O BCP. This leads to an increase in the proton transfer energy barrier for the NH…O tautomeric form, and the contribution of the bond between A and B atoms ($q(A|B)$) confirms this idea. Thus, at the end of this section, we have come to the same results that were described in other sections: two sites of the IPT (1 and 2) are the same and the dihedral angles have no effect on the barrier energies and percenttage of the tautomers.

CONCLUSIONS

In this work, 3,3′-dihydroxy-4,4′-[4,4′-diphenylmethanebis(nitrilomethylidyne)]-bis-phenol has newly been synthesized and characterized experimentally by the elemental analysis, NMR and IR spectroscopies. The proposed formula for this Schiff base is in agreement with the experimental results. Four possible tautomers of the Schiff base were investigated computationally using the DFT methods.

The geometries of four possible tautomers of the investigated Schiff base were fully optimized, and **L1** was found to be the most stable one. None of the tautomers has a planar structure. The intramolecular hydrogen bonds increase the stability of the investigated tautomers.

In **L1**, the H1 and H2 phenolic protons are engaged in the intramolecular hydrogen bond (—O—H…N), which affects considerably their NMR chemical shifts and the energy of their O—H stretching vibration in the IR spectra, too.

Tautomerism of **L1** can occur in two different pathways (from sites 1 and 2). By a comparison of the electrostatic potential maps of several structures and the topological parameters by the AIMall package, it was finally concluded that the IPT reaction progress from two pathways was equially possible.

The calculated structural parameters are in agreement with the values reported for the similar compounds, confirming the validity of the optimized geometry. On the other hand, the obtained DFT results can be used for the identification of similar compounds.

REFERENCES

1. *Sevvel R., Rajagopal S., Srinivasan C., Ismail Alhaji N., Chellamani A.* // J. Org. Chem. – 2000. – **65**. – P. 3334 – 3340.
2. *Meunier B.* // Chem. Rev. – 1992. – **92**. – P. 1411 – 1456.
3. *Ostovic D., Bruice T.C.* // Acc. Chem. Res. – 1992. – **25**. – P. 314 – 320.
4. *Canali L., Sherrington D.C.* // Chem. Soc. Rev. – 1999. – **28**. – P. 85 – 93.
5. *Bahramian B., Mirkhani V., Moghadam M., Amin A.H.* // Appl. Catal., A. – 2006. – **315**. – P. 52 – 57.
6. *Palucki M., McCormick G.J., Jacobsen E.N.* // Tetrahedron Lett. – 1995. – **36**. – P. 5457 – 5460.
7. *Irie R., Hosoya N., Katsuki T.* // Synlett. – 1994. – P. 255 – 256.
8. *Linker T.* // Angew. Chem., Int. Ed. Engl. – 1997. – **36**. – P. 2060 – 2062.
9. *Hamada T., Fukuda H., Katsuki T.* // Tetrahedron. – 1996. – **52**. – P. 515 – 530.
10. *Gravert D.J., Griffin J.H.* // Inorg. Chem. – 1996. – **35**. – P. 4837 – 4847.
11. *Routier S.E., Bernier J.L., Warninig M.J., Colson P., Bailly C.* // J. Org. Chem. – 1996. – **61**. – P. 2326 – 2331.
12. *Eshtiagh-Hosseini H., Housaindokht M.R., Beyramabadi S.A., Beheshti S., Esmaeili A.A., Javan-Khoshkholgh M., Morsali A.* // Spectrochim. Acta, Part A. – 2008. – **71**. – P. 1341 – 1347.
13. *Eshtiagh-Hosseini H., Mirzaei M., Aghabozorg H., Beyramabadi S.A., Eshghi H., Morsali A., Shokrollahi A., Aghaei R.* // Spectrochim. Acta, Part A. – 2011. – **78**. – P. 1392 – 1396.
14. *Eshtiagh-Hosseini H., Housaindokht M.R., Beyramabadi S.A., Mir Tabatabaei S.H., Esmaeili A.A., Javan-Khoshkholgh M.* // Spectrochim. Acta, Part A. – 2011. – **78**. – P. 1046 – 1050.
15. *Beyramabadi S.A., Morsali A., Javan-Khoshkholgh M., Esmaeili A.A.* // Spectrochim. Acta, Part A. – 2011. – **83**. – P. 467 – 471.
16. *Beyramabadi S.A., Morsali A., Javan-Khoshkholgh M., Esmaeili A.A.* // J. Struct. Chem. – 2012. – **53**. – P. 460 – 467.
17. *Beyramabadi S.A., Morsali A., Shams A.R.* // J. Struct. Chem. – 2015. – **56**, N 2. – P. 259 – 265.
18. *Eshtiagh-Hosseini H., Beyramabadi S.A., Morsali A., Mirzaei M., Salimi A.R., Naseri M.A.* // J. Struct. Chem. – 2013. – **54**. – P. 1063 – 1069.
19. *Lee C., Yang W., Parr R.G.* // Phys. Rev. B. – 1988. – **37**. – P. 785 – 789.
20. *Frisch M.J. et al.* Gaussian 03, Revision B.03, Gaussian Inc., Pittsburgh, PA, 2003.
21. *Ditchfield R.* // Mol. Phys. – 1974. – **27**. – P. 789 – 807.
22. *Young D.C.* Computational Chemistry: A Practical Guide for Applying Techniques to Real-World Problems, John Wiley & Sons Inc., 2001.
23. *Bader R.F.W.* Atoms in Molecules: A Quantum Theory. – Oxford: Clarendon Press, 1994.
24. *Biegler-König F., Schönbohm J., Bayles D.* // J. Comput. Chem. – 2001. – **22**. – P. 545 – 559.
25. *Srinivasan K., Michaud P., Kochi J.K.* // J. Amer. Chem. Soc. – 1986. – **108**. – P. 2309 – 2320.
26. *Ma C.-B., Chen F., Chen C.-N., Liu Q.-T.* // Acta Crystallogr. – 2003. – **C59**. – P. m516 – m518.
27. *Huang D.-G., Zhang X.-F., Zhu H.-P., Chen C.-N., Liu Q.-T.* // Acta Crystallogr. – 2001. – **E57**. – P. m441 – m443.
28. *Butcher R.J., Towns W.* // Acta Crystallogr. – 2005. – **E61**. – P. m2618 – m2620.
29. *Martínez D., Motevalli M., Watkinson M.* // Acta Crystallogr. – 2002. – **C58**. – P. m258 – m260.
30. *Ni Z.-H., Kou H.-Z., Zhang L.-F., Jiang Y.-B., Cui A.-L.* // Acta Crystallogr. – 2005. – **E61**. – P. m796 – m798.
31. *Gwaram N.S., Khaledi H., Ali H.M.* // Acta Crystallogr. – 2010. – **E66**. – P. m813.
32. *Pui A., Policar C., Mahy J.-P.* // Inorg. Chim. Acta. – 2007. – **360**. – P. 2139 – 2144.
33. *Takjoo R., Centore R., Hakimi M., Beyramabadi S.A., Morsali A.* // Inorg. Chim. Acta. – 2011. – **371**. – P. 36 – 41.

34. *Leyton P., Paipa C., Berrios A., Zárate A., Castillo M.V., Brandán S.A.* // J. Mol. Struct. – 2013. – **1031**. – P. 110 – 118.
35. *Proft F.D., Geerlings P.* // Chem. Rev. – 2001. – **101**. – P. 1451 – 1464.
36. *Sanmartín J., García-Deibe A.M., Fondo M., Navarro D., Bermejo M.R.* // Polyhedron. – 2004. – **23**. – P. 963 – 967.
37. *Ware D.C., Mackie D.S., Brothers P.J., Denny W.A.* // Polyhedron. – 1995. – **14**. – P. 1641 – 1646.
38. *Li X.Y., Wang Y., Zheng S.J., Meng L.P.* // Struct. Chem. – 2012. – **23**. – P. 1233 – 1240.
39. *Bader R.* Atoms in Molecules: A Quantum Theory. – Oxford: Clarendon, UK, 1990.
40. *Filarowski A., Majerz I.* // J. Phys. Chem. A. – 2008. – **112**. – P. 3119 – 3126.
41. *Espinosa E., Souhassou M., Lachekar H., Lecomte C.* // Acta Crystallogr., Sect. B: Struct. Sci. – 1999. – **55**. – P. 563 – 572.
42. *Grabowski S.J.* // J. Phys. Chem. A. – 2000. – **104**. – P. 5551 – 5557.
43. *Jenkins S., Morrison I.* // Chem. Phys. Lett. – 2000. – **317**. – P. 97 – 102.
44. *Mariam Y.H., Musin R.N.* // J. Phys. Chem. A. – 2008. – **112**. – P. 134 – 145.
45. *Carroll M.T., Bader R.F.* // Mol. Phys. – 1988. – **65**. – P. 695 – 722.
46. *Ángyán J.G., Loos M., Mayer I.* // J. Phys. Chem. – 1994. – **98**. – P. 5244 – 5248.
47. *Kolandaivel P., Nirmala V.* // J. Mol. Struct. – 2004. – **694**. – P. 33 – 38.
48. *Gatti C., Saunders V.R., Roetti C.* // J. Chem. Phys. – 1994. – **101**. – P. 10686 – 10696.
49. *Grabowski S.J.* // J. Mol. Struct.: THEOCHEM. – 2007. – **811**. – P. 61 – 67.